0026-895X/96/030639-11$3.00/0

MOLECULAR PHARMACOLOGY, 50:639–649 (1996).

Interactions of Oxime Reactivators with Diethylphosphoryl Adducts of Human Acetylcholinesterase and Its Mutant Derivatives

HAIM GROSFELD, DOV BARAK, ARIE ORDENTLICH, BARUCH VELAN, and AVIGDOR SHAFFERMAN

Departments of Biochemistry (H.G., A.O., B.V., A.S.) and Organic Chemistry (D.B.), Israel Institute for Biological Research, Ness-Ziona 70450, Israel

Received December 13, 1995; Accepted May 3, 1996

SUMMARY

Diethylphosphoryl conjugates of human acetylcholinesterase (AChE) and selected mutants, carrying amino acid replacements at the active center and at the peripheral anionic site, were subjected to reactivation with the monopyridinium oxime 2-hydroxy-iminomethyl-1-methylpyridinium chloride and the bispyridinium oximes 1,3-bis(4′-hydroxyiminomethyl-1′-pyridinium),propane dibromide (TMB-4) and 1-(2′-hydroxyiminomethyl-1′-pyridinium)-3-(4″-carbamoyl-1″-pyridinium)-2-oxapropane dichloride (HI-6). The kinetic profiles for all of the reactivation reactions indicate single populations of reactivatable species. Replacement of Trp86, the anionic subsite in the active center, lowered the affinity of the free enzyme toward all three reactivators, but in the corresponding diethylphosphoryl conjugate, only affinity toward TMB-4 was affected. Replacement of other constituents of the hydrophobic subsite (Tyr337, Phe338) had no major effect on either affinity to the free enzymes or rates of reactivation. Substitution of residues of the acyl pocket (Phe295, Phe297) lowered the affinities toward reactivators except for the 20-fold increase in affinity of F295A toward HI-6. Replacement of the acidic residues in the active center (Glu202, Glu450) affected mainly the rates of nucleophilic displacement of the phosphoryl moiety. The effect of substituting residues constituting the peripheral anionic site at the rim of the active site gorge (Tyr72, Asp74, Trp286) was particularly puzzling because for 2-hydroxy-iminomethyl-1-methylpyridinium chloride and HI-6, mainly the nucleophilic reaction rate constants were affected, whereas for TMB-4, the affinities of the phosphorylated enzymes were significantly reduced. The fact that perturbations of the functional architecture of HuAChE active center can account for only some of the observed effects on the reactivation rates suggests that the binding modes of oxime to the phosphorylated and nonphosphorylated enzymes are considerably different and/or that interactions of the reactivators with the phosphoryl moieties play a dominant role in the reactivation process.

AChE (EC 3.1.1.7), a key enzyme in cholinergic transmission, is the major target of poisoning by organophosphorus agents through phosphylation[1] at the catalytic serine. Inactivation of AChE leads to an overstimulation of cholinergic receptors and symptoms such as salivation, tremors, and miosis and, at greater doses of the phosphylating agent, to respiratory paralysis and death (1). The phosphylated AChE may undergo spontaneous reactivation by hydrolytic displacement of the phosphyl moiety from the enzyme; however, this is usually a slow and inefficient process of no practical significance (2). Alternatively, such displacement can be readily accomplished by an appropriate nucleophile like fluoride or an oxime to generate a reactivated enzyme molecule (3, 4). Thus, AChE reactivation by certain oximes is an important part of the treatment in cases of human poisoning by organophosphorus derivatives such as insecticides or warfare nerve agents (5, 6). Despite the therapeutic significance of the oxime reactivators and notwithstanding the considerable effort invested in development of new derivatives, surprisingly little is known about the structure-activity relationship associated with the reactivation process. Reactivators like the monoquaternary 2-PAM (the methanesulfonate salt is known as P2S) and the bisquaternary TMB-4 are particularly effective in reactivating phosphorylated AChEs and relatively ineffective in reactivating phosphonyl conjugates (7, 8). On the other hand, HI-6 is more effective in reactivating phosphonylated AChEs that result from exposure to potent organophosphorus inhibitors such as sarin and soman

This work was supported by the U.S. Army Research and Development Command Contract DAMD17-93-C-3042 (A.S.).

[1] The comprehensive term "phosphyl" is adopted from Bourne and Williams (40) for all tetravalent P electrophilic groups.

ABBREVIATIONS: AChE, acetylcholinesterase; HuAChE, human acetylcholinesterase; ATC, acetylthiocholine; 2-PAM, 2-hydroxy-iminomethyl-1-methylpyridinium chloride; TMB-4, 1,3-bis(4′-hydroxyiminomethyl-1′-pyridinium),propane dibromide; HI-6, 1-(2′-hydroxyiminomethyl-1′-pyridinium)-3-(4″-carbamoyl-1″-pyridinium)-2-oxapropane dichloride; PAS, peripheral anionic site.

(7, 9). The apparent lack of correlation between the structural features of the reactivators and their reactivation efficiencies is a major obstacle to the development of novel advantageous oxime reactivators.

The resolution of the X-ray structure of AChE (10) together with extensive site-directed mutagenesis studies on recombinant enzyme molecules (11–20) has opened a new avenue to investigate structure-function features of AChE reactivity. This has led to the dissection of the active center architecture (15–17, 20), analysis of the involvement of the periphery in HuAChE reactivity (14, 18, 20, 21), and examination of the phosphorylation (22), aging (23), and reactivation (24) processes.

We report on the application of this approach to gain insight into the reactivation of phosphorylated HuAChE. We examined the reactivity of three structurally distinct reactivators toward phosphorylated HuAChE and selected derivatives of this enzyme, in which critical residues were replaced by site-directed mutagenesis. The thorough kinetic studies unravel some of the characteristics of the reactivation process yet also indicate that the reactivity patterns of phosphylated HuAChE enzyme toward oxime reactivators are more complex than originally thought.

Materials and Methods

Generation of HuAChE mutants. HuAChE mutants Y72A(*70*),[2] D74N(*72*), W86A(*84*), E202A, E202Q(*199*), W286A(*279*), F295A(*288*), F297A(*290*), Y337A, Y337F(*F330*), F338A(*331*), E450A(*443*), and the double mutant Y72A/W286A were generated as described previously (12, 14, 16, 18, 22). The HuAChEs were expressed in the human embryonal kidney 293 cell line (25, 26). Stable recombinant cell clones expressing high levels of wild-type and mutant AChEs were propagated in multitray systems (27), and enzymes were purified (>90% purity) either by ligand affinity chromatography (26) or by fractionation on monoclonal antibody affinity columns (28).

Analysis of AChE activity. All kinetic studies were carried out with ATC (Sigma Chemical, St. Louis, MO) as substrate (29). Standard assays were performed in the presence of 0.2 mg/ml bovine serum albumin, 0.3 mM 5,5′-dithiobis(2-nitrobenzoic acid), 50 mM sodium-phosphate buffer, pH 8.0, and 0.5 mM ATC or other concentrations as indicated (total solution volume was 100 μl). The assays were carried out at 27° and monitored by a Thermomax microplate reader (Molecular Devices, Sunnyvale, CA). The inhibitor paraoxon (*O*,*O*-diethyl-*O*-(4-nitrophenyl)-phosphate) and the reactivator 2-PAM were purchased from Sigma. The reactivators TMB-4 and HI-6 were a gift from Dr. G. Amitai and Dr. L. Raveh (Department of Pharmacology, Israel Institute for Biological Research, Ness-Ziona, Israel) (for chemical formulas, see Fig. 1).

Reactivation of paraoxon-inhibited HuAChE. Paraoxon was used to completely inhibit the AChEs as the preceding step to the reactivation assay. This organophosphate was selected because its AChE adduct does not undergo significant aging, a process that involves dealkylation of the phosphylated AChE, leading to a nonreactivatable conjugate, within the time frame of the reactivation experiments. The amounts of paraoxon required for inhibition of the various HuAChE enzymes were calculated by using the predetermined apparent bimolecular rate constants for the phosphorylation of wild-type HuAChE and of each of its mutants (22). Routinely, two identical aliquots of ~3 U of AChE in 0.1 ml were used: one was inhibited with paraoxon, and the other served as a control. After inhibition, an aliquot of each of the reaction mixtures was diluted in buffer (50 mM phosphate buffer, pH 8.0, supplemented with 0.2 mg/ml of bovine serum albumin) and assayed to verify inhibition (>98%). Excess of unreacted inhibitor was immediately removed from the enzyme preparation by centrifugation through a 3-ml Sephadex G-15 spin column (3-min spin at 2500 rpm). The control noninhibited enzyme preparation was treated similarly. The flow-through fractions containing the enzyme were diluted to a final working concentration of 0.3 U/ml. In all cases, the spin column treatment proved to eliminate all inhibitory activity from the paraoxon-treated samples, as verified by spiking with AChE. Reactivation reactions were initiated by the addition of the various oximes (concentrations, 0.001–2.0 mM) to the paraoxon-free enzyme solutions in 50 mM phosphate buffer, pH 8.0, and were carried out at 27°. Regeneration of AChE activity was monitored by diluting 10-μl samples of the reactivation mixture into 100 μl of the assay solution containing ATC and 5,5′-dithiobis(2-nitrobenzoic acid, and the enzymatic reaction was followed for 3–5 min, allowing 7–11 time point readings. Control noninhibited enzyme preparations and samples without enzyme were treated similarly and were used for estimation of the expected enzyme activity at maximal reactivation and for monitoring the background readings, respectively. The contribution of spontaneous reactivation was estimated by monitoring the enzymatic activity of paraoxon-inhibited enzyme samples in the absence of reactivator.

Analysis of the kinetic data. According to Green and Smith (30), the reactivation process can be kinetically described by the two steps shown in equation 1:

$$E(OP) + R \underset{k_{-1}}{\overset{k_1}{\rightleftharpoons}} E(OP)\cdot R \xrightarrow{k_2} E + R(OP) \quad (1)$$

In equation 1, E(OP) is the inhibited enzyme, R is the reactivator, E(OP)·R is the intermediate complex, E is the free enzyme, and R(OP) is the phosphorylated reactivator. All of the reactivation experiments described here were performed under pseudo-first-order conditions with respect to the reactivator ($[R] \gg [E(OP)]_0$).

According to equation 1, the time-dependent change of phosphorylated enzyme concentration is provided by equation 2, where K_r can be considered as the dissociation constant of the complex E(OP)·R under the condition $k_{-1} \gg k_2$. From equation 2, the relation between k_{obs} (the experimental rate constant of reactivation) and the kinetic constants K_r and k_2 is described by equation 3:

$$\ln \frac{[E(OP)]_0}{[E(OP)]_t} = \left\{ \frac{\frac{k_2}{K_r}[R]}{1 + \frac{[R]}{K_r}} \right\} t = k_{obs} t \quad (2)$$

$$\frac{1}{k_{obs}} = \frac{K_r}{k_2} \times \frac{1}{[R]} + \frac{1}{k_2} \quad (3)$$

$$\ln\left(1 - \frac{[E]_t}{[E]_\infty}\right) = -k_{obs} t \quad (4)$$

In these equations, the subscripts 0, t, and ∞ correspond to the respective values at zero time, at time t, and after complete reactivation. Because $[E(OP)]_t = [(EOP)]_0 - [E]_t$ and because under conditions of complete reactivation $[E(OP)]_0 = [E]_\infty$, the concentrations in equation 2 can be expressed in terms of the reactivated enzyme (equation 4). Accordingly, values for the dissociation constant K_r and the dephosphorylation rate constant k_2 can be derived by determining k_{obs} at different reactivator concentrations (according to equation 3), followed by plotting the double reciprocal relation of k_{obs} versus [R] (according to equation 3). From these linear plots, one can determine the ratios of K_r/k_2 from the slopes, which are equivalent to the reciprocal values of the apparent bimolecular rate constants of reactivation k_r, and values of k_2 from the *y*-intercepts. The constants k_r

[2] Amino acids and numbers refer to HuAChE, and the numbers in parentheses refer to the positions of analogous residues in *Torpedo californica* acetylcholinesterase according to the recommended nomenclature (41).

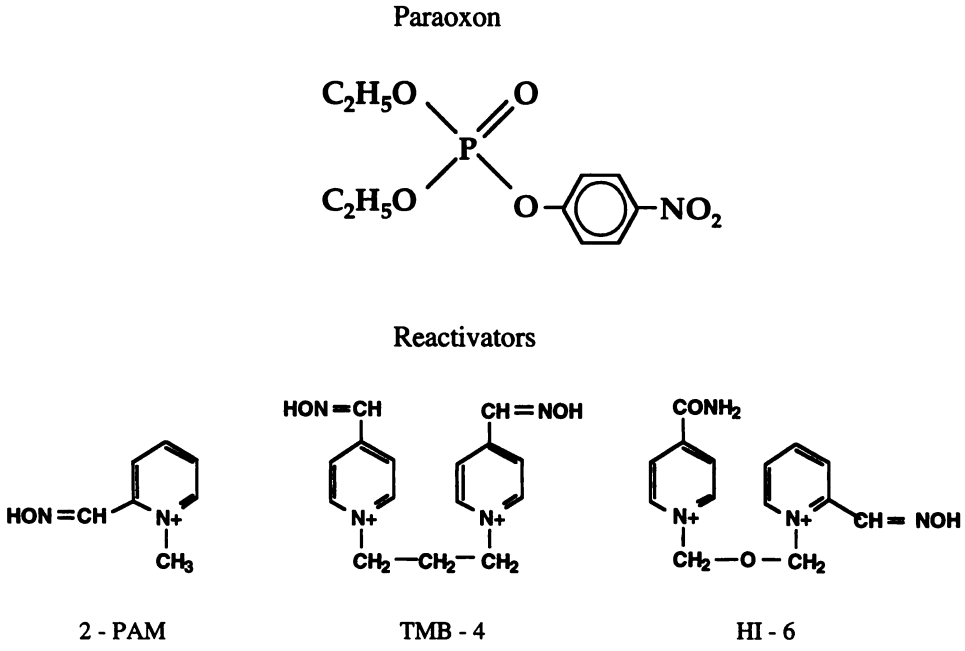

Fig. 1. Chemical formulas of the inhibitor and the reactivators used in this study.

have also been referred to as bimolecular reaction constants because they include equilibrium as well as rate constants (31).

Treatment of side reactions accompanying the reactivation reaction. The relative difficulty in determining kinetic constants from the reactivation assay is a consequence of the multiple reactions that may occur simultaneously and must be either eliminated if possible or considered in the evaluation of the data to avoid erroneous interpretation of the results.

$$E + R \overset{K_{ox}}{\rightleftharpoons} E \cdot R \quad (5a)$$

$$R + (OP) \rightarrow R(OP) \quad (5b)$$

$$R(OP) + E \rightarrow E(OP) + R \quad (5c)$$

$$S + R \rightarrow \text{hydrolysis products} \quad (5d)$$

$$E(OP) \rightarrow E + OP \quad (5e)$$

An underestimation of the reactivation rate due to a reversible inhibition by the reactivator (equation 5a) of the newly reactivated free enzyme was avoided by including identical concentrations of reactivator in the noninhibited control enzyme preparation. The phosphorylated reactivator R(OP) is a potential phosphorylating agent of the reactivated enzyme (equation 5, b and c). The direct phosphorylation of the reactivator was avoided by efficient removal of the excess of paraoxon, as described above. This allowed minimisation of the formation of R(OP) during reactivation to a concentration equivalent to that of the reactivated enzyme. To correct for possible hydrolysis of substrate ATC (S) due to oxime-induced reaction (equation 5d), we included the appropriate blanks. Such correction was important mainly in case of diethylphosphoryl-W86A due to the high concentration of ATC needed to monitor the activity of the free enzyme. Spontaneous reactivation of the inhibited enzyme (equation 5e) was not observed in our experiments.

Determination of the inhibition constants of HuAChE enzymes by oxime reactivators. Values of the reversible inhibition constants (K_{ox}) were determined by monitoring the effects of various oxime concentrations on the rate of the enzymatic hydrolysis of ATC. For each concentration of oxime (0.1–0.8 mM), the hydrolysis was carried out with various ATC concentrations (0.03–3.75 mM) in phosphate buffer, pH 8.0, containing 0.3 mM DTNB. In each case, the enzymatic reaction was monitored for 5 min, allowing 11 time point readings within the Thermomax linear range. Values of K_{ox} were obtained from the double reciprocal plots of the slopes derived from Lineweaver-Burk plots versus the concentration of the inhibitor (20). In case of W86A, concentration of ATC was increased to 25 mM, resulting in high background product levels in the presence of the reactivators. All activities were corrected for oxime-induced hydrolysis of ATC.

Results

Kinetics of reactivation of paraoxon-inhibited HuAChE. The lack of a consistent structure-function relationship makes it difficult to formulate a reliable mechanistic scheme for the oxime-induced reactivation reaction. The most frequently used reactivation model implicates formation of a noncovalent complex between the phosphylated enzyme and the reactivator, followed by a nucleophilic displacement of the phosphyl moiety (equation 1). Nevertheless, kinetic results from many reactivation studies provide only partial support for this model (32). This may be a consequence of experimental difficulties due to the aging process and other side reactions that compete with the reactivation (see equation 5).

To evaluate the reactivation kinetics of phosphorylated HuAChE and, in particular, of the phosphorylated mutants, which are less amenable to reactivation, we used an assay system in which these side reactions are either eliminated or corrected for (see Materials and Methods). The reactivation process was monitored using HuAChE enzymes inhibited by paraoxon (see Fig. 1). The resulting diethylphosphoryl adducts are not susceptible to the aging process during the time course of the experiments (2) and are achiral with respect to the phosphorous atom and consequently should provide a homogeneous population of reactivatable species.

To evaluate the effect of structural modifications of the enzyme on interaction with reactivators, three different oximes (Fig. 1) representing the monopyridinium (2-PAM) and bispyridinium (TMB-4 and HI-6) reactivator classes were used. Among the two bispyridinium compounds, HI-6

represents the Hagedorn-type reactivators known to be particularly reactive toward AChEs inhibited by phosphonates, whereas TMB-4 is more effective in reactivation of phosphoryl-AChEs (7–9). This dependence of reactivation efficiency for the two structurally related oximes on the structure of the AChE-bound phosphyl moiety is still not clearly understood (8).

Reactivation of phosphorylated HuAChE proceeds to completion with any of the oximes selected, and curve fitting of the kinetic data (according to $E_t = E_\infty(1 - e^{-tk_{obs}})$; see equation 4) exhibits a monoexponential dependence (Fig. 2A). The same kinetic behavior has been observed for adducts in which reactivation is efficient as well as for cases in which the reaction is very slow as exemplified by the oxime-induced reactivation reactions of phosphorylated D74N, E202Q, and W86A HuAChEs (Fig. 3). The kinetics profiles, observed for reactivation of diethylphosphoryl adducts of all of the HuAChE mutants tested in this study, were linear (r = 0.965–0.998), indicating that the population of reactivatable species is indeed homogeneous and that the assay conditions, which we selected, effectively eliminate interference from competing reactions (see equation 5). We note that nonlinear behavior was experienced only with the use of exceedingly high concentrations of reactivator. Such linear behavior also supports the proposed reactivation kinetic scheme (equation 1), under the conditions studied, and therefore the values of k_r, K_r, and k_2 can serve as an adequate measure of the enzyme reactivity characteristics toward the reactivators examined.

The oxime reactivators are also inhibitors of the nonphosphorylated HuAChE enzymes, presumably by binding at the active center through interactions of the charged pyridinium moieties (33). To compare the affinities of the free and diethylphosphoryl-HuAChEs toward the reactivators, as well as to correct for the reversible inhibition of the reactivated enzyme (see Materials and Methods), the inhibition constants K_{ox} were evaluated. The affinity of the diethylphosphoryl-HuAChE enzymes toward the reactivators is approximated by the values of K_r. According to equation 1, $K_r = (k_{-1} + k_2)/k_1$; however, because the measured values of k_2 are within the range of 0.065–6.5 $\times 10^{-2}$ min^{-1} (see Tables 1–3), it follows that $k_{-1} \gg k_2$ or that $K_r \approx k_{-1}/k_1$ (k_{-1} is estimated to be in the range of 10^4–10^6 min^{-1} based on the assumption that the association proceeds at close to diffusion controlled rates and on the measured values of K_r). Examination of the values of K_{ox} and K_r for the free and the diethylphosphoryl-HuAChE revealed that although the affinity of TMB-4 toward the phosphorylated enzyme is 30-fold higher than that toward the free HuAChE, the opposite was true for HI-6, with the affinity toward the phosphorylated enzyme being 16-fold lower. For 2-PAM, the corresponding affinities were comparable (as reported also for P2S; see Ref. 31). Furthermore, the affinity of TMB-4 toward the phosphorylated HuAChE was

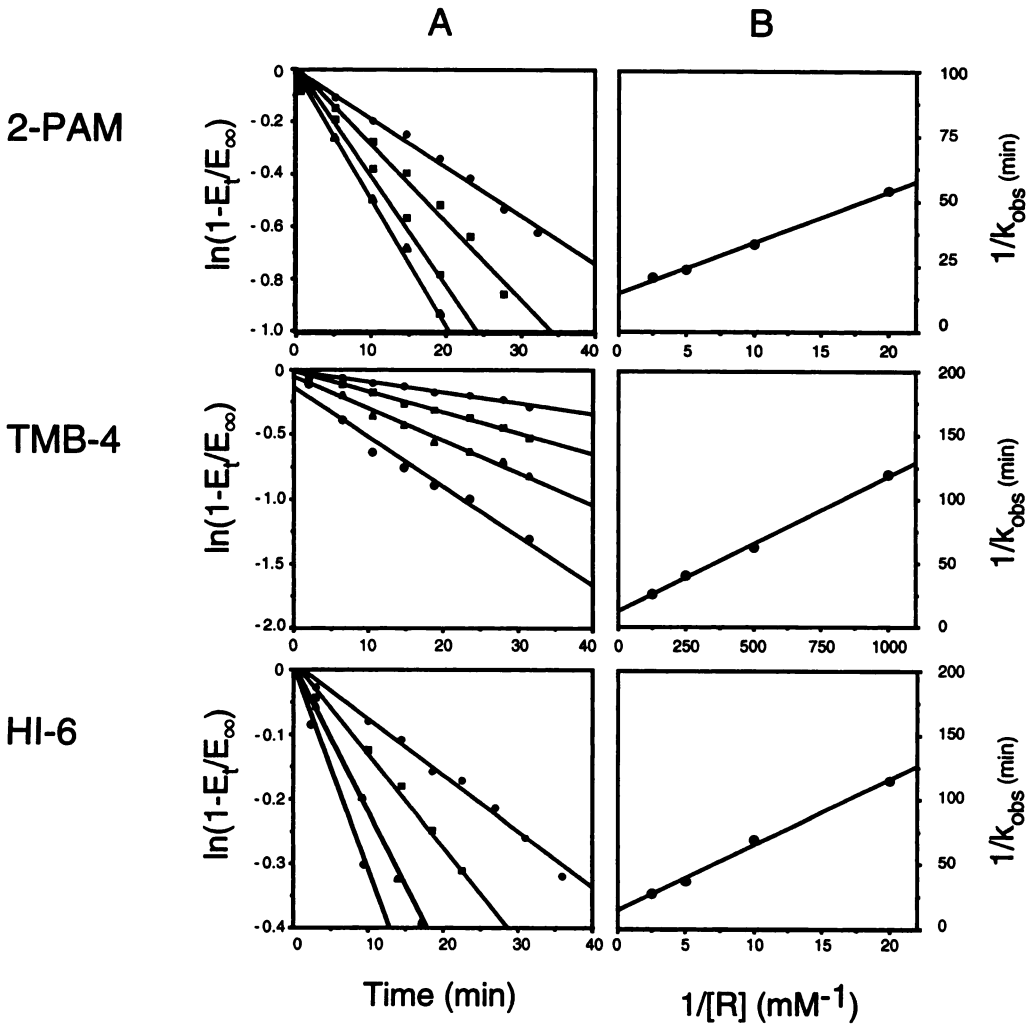

Fig. 2. Determination of the kinetic constants k_r, K_r, and k_2 for reactivation of diethylphosphoryl-HuAChE by 2-PAM, TMB-4, and HI-6. A, Semilogarithmic plots of the relative concentrations of the reactivated enzyme versus reaction time for four concentrations of reactivator in the following ranges: 2-PAM, 0.05–0.4 mM; TMB-4, 0.001–0.008 mM; and HI-6, 0.05–0.4 mM. Values of k_{obs} were estimated from the slopes. B, Double reciprocal plots of k_{obs} versus reactivator concentration (see equation 2), yielding the values of $K_r/k_2(1/k_r)$ from the slopes and values of $1/k_2$ from the y-intercepts.

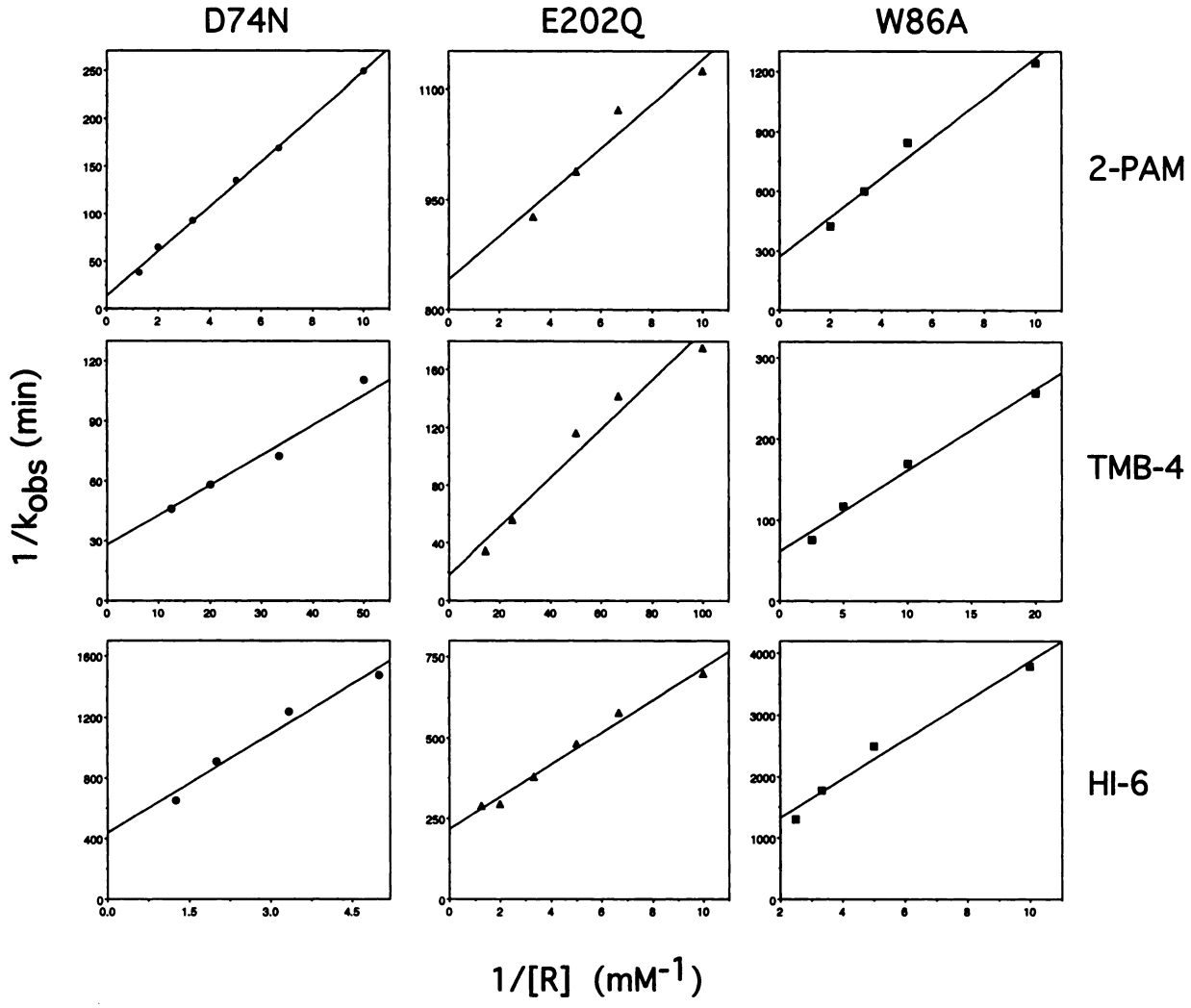

Fig. 3. Representative double reciprocal plots of k_{obs} versus reactivator concentration for selected HuAChE mutant derivatives. Reactivations of phosphorylated HuAChE enzymes mutated at the H-bond network (E202Q), the active center anionic subsite (W86A), and the PAS (D74N) by the reactivators 2-PAM, TMB-4, and HI-6 are shown.

much higher than those of either 2-PAM or HI-6, accounting for the superior efficiency of TMB-4 as reactivator because the values of k_2 were comparable for the three oximes.

Effect of amino acid replacements at the active center on reactivation. The selection of HuAChE mutants for the study was based primarily on the assumption that the reactivators interact with the enzyme at its active center. Accordingly, mutants carrying substitution of residues constituting the hydrophobic pocket (Trp86, Tyr337, Phe338), residues of the acyl pocket (Phe295, Phe297) and residues implicated in the hydrogen bond network (Glu202, Glu450) (13, 15–17, 19, 20) were investigated.

The tryptophan at position 86 is involved in stabilization of the charge in the enzyme substrate (Michaelis-Menten) complex, and its replacement results in a drastic loss of affinity toward charged AChE ligands such as edrophonium or decamethonium (16, 20). It could be therefore expected that this residue would interact with the charged pyridinium moieties of the oxime reactivators; in the recently resolved X-ray structure of 2-pyridinium aldoxime/*Torpedo californica* acetylcholinesterase complex,[3] the pyridinium moiety is stacked against the indole ring of Trp84 (residue equivalent to Trp86 in HuAChE). Indeed, replacement of Trp86 by alanine results in a considerable decrease in affinity of the nonphosphorylated W86A HuAChE toward all three reactivators tested, as demonstrated by the corresponding values of K_{ox} (Tables 1–3). In contrast, and quite surprisingly, the effects of this mutation on the affinity of the diethylphosphoryl-W86A toward 2-PAM and HI-6, relative to those of the phosphorylated wild-type HuAChE, are negligible. For all of the three reactivators, a decrease in capacity to reactivate the phosphorylated W86A enzyme, relative to the wild-type HuAChE, is evident from the respective k_r values. However, for 2-PAM and HI-6, this is mainly due to a decrease in k_2, whereas for TMB-4, it is predominantly an outcome of impaired binding to the diethylphosphoryl-W86A HuAChE. Nevertheless, one should note that the affinity of diethylphosphoryl-W86A toward TMB-4 is still greater than that of the corresponding nonphosphorylated enzyme.

Residues Phe338 and Tyr337 together with Trp86 are believed to constitute the hydrophobic pocket, accommodating one of the alkoxy substituents of the phosphoryl moiety and also the leaving group in paraoxon/HuAChE Michaelis complex (22). Due to its location, above the phosphorous and

[3] J. Sussman, personal communication.

TABLE 1

Kinetic constants for reactivation by 2-PAM

Values are mean ± standard error from at least four determinations. Values of the apparent bimolecular rate constants of reactivation k_r and of the first-order rate constant k_2 and were obtained from the slopes and y-intercepts of the double reciprocal relations of k_{obs} versus [R]. K_r values were calculated from the ratio $K_r = k_2/k_r$ for each determination, and the corresponding standard error values represent deviations from the calculated mean. Inhibition constants of the free enzymes by the reactivators K_{ox} were derived from Lineweaver-Burk plots (see Materials and Methods).

Enzyme	k_r	$k_2 \times 10^2$	K_r	K_{ox}
	$M^{-1}\ min^{-1}$	min^{-1}	mM	mM
Wild-type	460 ± 70	6.0 ± 0.82	0.13 ± 0.01	0.28 ± 0.03
W86A	10 ± 4	0.3 ± 0.08	0.3 ± 0.07	>2[a]
F295A	180 ± 27	1.0 ± 0.15	0.06 ± 0.02	1.0 ± 0.15
F297A	134 ± 43	3.0 ± 0.9	0.21 ± 0.1	0.9 ± 0.05
Y337A	220 ± 39	6.0 ± 0.15	0.27 ± 0.04	0.76 ± 0.05
Y337F	510 ± 150	2.5 ± 0.7	0.05 ± 0.02	1.0 ± 0.2
F338A	180 ± 29	5.4 ± 0.35	0.30 ± 0.06	0.59 ± 0.17
E202A	15 ± 5	1.2 ± 0.22	0.80 ± 0.22	0.44 ± 0.08
E202Q	41 ± 5	0.16 ± 0.04	0.04 ± 0.01	0.46 ± 0.04
E450A	60 ± 25	0.4 ± 0.09	0.07 ± 0.03	1.0 ± 0.03
Y72A	80 ± 27	0.8 ± 0.18	0.1 ± 0.02	0.63 ± 0.1
W286A	55 ± 12	0.8 ± 0.15	0.14 ± 0.02	0.43 ± 0.05
Y72A/W286A	100 ± 16	1.0 ± 0.2	0.1 ± 0.006	0.67 ± 0.07
D74N	47 ± 7	7.0 ± 0.73	1.5 ± 0.11	1.2 ± 0.08

[a] Only the lower limit could be estimated due to high background (see Materials and Methods).

TABLE 2

Kinetic constants for reactivation by TMB-4

Values are mean ± standard error from at least four determinations. Values of the apparent bimolecular rate constants of reactivation k_r and of the first-order rate constant k_2 and were obtained from the slopes and y-intercepts of the double reciprocal relations of k_{obs} versus [R]. K_r values were calculated from the ratio $K_r = k_2/k_r$ for each determination, and the corresponding standard error values represent deviations from the calculated mean. Inhibition constants of the free enzymes by the reactivators K_{ox} were derived from Lineweaver-Burk plots (see Materials and Methods).

Enzyme	k_r	$k_2 \times 10^2$	K_r	K_{ox}
	$M^{-1}\ min^{-1}$	min^{-1}	mM	mM
Wild-type	10000 ± 1420	6.0 ± 0.55	0.007 ± 0.0008	0.21 ± 0.03
W86A	150 ± 25	3.1 ± 0.07	0.2 ± 0.03	>2[a]
F295A	610 ± 62	0.3 ± 0.045	0.005 ± 0.002	0.11 ± 0.02
F297A	1200 ± 190	3.6 ± 1.8	0.03 ± 0.013	0.73 ± 0.1
Y337A	3400 ± 360	3.0 ± 0.5	0.009 ± 0.003	0.06 ± 0.018
Y337F	8000 ± 1250	3.0 ± 0.6	0.004 ± 0.001	0.32 ± 0.08
F338A	3100 ± 460	0.9 ± 0.17	0.003 ± 0.0009	0.17 ± 0.022
E202A	170 ± 17	0.32 ± 0.09	0.018 ± 0.007	0.18 ± 0.02
E202Q	580 ± 25	4.0 ± 1	0.07 ± 0.02	0.20 ± 0.03
E450A	340 ± 78	1.0 ± 0.3	0.03 ± 0.008	0.39 ± 0.0017
Y72A	460 ± 56	4.4 ± 0.3	0.1 ± 0.01	0.3 ± 0.04
W286A	360 ± 20	4.0 ± 0.6	0.11 ± 0.009	0.26 ± 0.023
Y72A/W286A	50 ± 19	3.0 ± 0.7	0.6 ± 0.15	1.10 ± 0.3
D74N	660 ± 32	4.6 ± 1.3	0.07 ± 0.02	0.57 ± 0.12

[a] Only the lower limit could be estimated due to high background (see Materials and Methods).

opposite the P—O—Ser203 bond, this subsite could play a role in the juxtaposing the nucleophilic moiety of the reactivator with the phosphoryl moiety. Contrary to this prediction, substitution of neither Tyr337 nor Phe338 by alanine had a major effect on the bimolecular reactivation rate constants or on the affinity of the nonphosphorylated enzymes toward the reactivators (Table 1–3). The only effects worth noting are related to the affinities of the phosphorylated F338A mutant for both TMB-4 and HI-6, which are higher than the corresponding values for the wild-type enzyme. However, this affinity increase is not reflected in the k_r values because a concomitant decrease in k_2 is observed for the same two reactivators.

Residues Phe295 and Phe297 were shown to constitute the binding site for the acyl moiety of AChE substrates and for the alkoxy group of the organophosphorus inhibitors (15, 16, 20). Substitution at these positions resulted in different changes of the reactivation rate constants for the different reactivators (Tables 1–3). Replacement of Phe297 by alanine resulted in a moderate decrease in affinity toward all of the reactivators tested by both the phosphorylated and the free enzymes. The reactions of diethylphosphoryl-F295A HuAChE with 2-PAM and TMB-4 reveal a significant decrease in the bimolecular rate constants of reactivation resulting only from reduced values of k_2. This is not the case for HI-6, where surprisingly a 7-fold increase of affinity toward the phosphorylated enzyme was observed (Tables 1–3). Consequently, a 3-fold increase of the corresponding value of k_r was observed, although the decrease in the value of k_2 is comparable to that of 2-PAM. The nonuniform effects of replacement at position 295 could result from the relative positioning of the diethylphosphoryl moiety in the phosphorylated F295A enzyme.

The precise positioning of the Glu202 carboxylate is an important feature of the functional architecture of the HuAChE active center (20, 22). Such positioning is achieved through an H-bond network spanning the cross section of the active site gorge and including residues Glu450 and Tyr133 and the backbone amide oxygens of Gly122 and Gly448. Perturbation

TABLE 3

Kinetic constants for reactivation by HI-6

Values are mean ± standard error from at least four determinations. Values of the apparent bimolecular rate constants of reactivation k_r and of the first-order rate constant k_2 and were obtained from the slopes and y-intercepts of the double reciprocal relations of k_{obs} versus [R]. K_r values were calculated from the ratio $K_r = k_2/k_r$ for each determination, and the corresponding standard error values represent deviations from the calculated mean. Inhibition constants of the free enzymes by the reactivators K_{ox} were derived from Lineweaver-Burk plots (see Materials and Methods).

Enzyme	k_r	$k_2 \times 10^2$	K_r	K_{ox}
	$M^{-1}\ min^{-1}$	min^{-1}	mM	mM
Wild-type	170 ± 46	6.0 ± 0.2	0.35 ± 0.1	0.022 ± 0.004
W86A	7 ± 3	0.4 ± 0.2	0.55 ± 0.15	>2[a]
F295A	520 ± 20	2.6 ± 1.0	0.05 ± 0.005	0.19 ± 0.006
F297A	22 ± 5	2.0 ± 0.9	1.0 ± 0.6	0.27 ± 0.012
Y337A	120 ± 15	2.4 ± 0.28	0.2 ± 0.03	0.14 ± 0.02
Y337F	113 ± 52	4.0 ± 1.2	0.34 ± 0.13	0.12 ± 0.02
F338A	80 ± 20	0.55 ± 0.05	0.07 ± 0.02	0.044 ± 0.004
E202A	5 ± 1	0.065 ± 0.03	0.13 ± 0.05	0.05 ± 0.001
E202Q	19 ± 10	0.45 ± 0.12	0.22 ± 0.12	0.05 ± 0.008
E450A	4.0 ± 0.3	0.056 ± 0.01	0.14 ± 0.006	0.39 ± 0.01
Y72A	24 ± 8	1.2 ± 0.2	0.5 ± 0.15	0.06 ± 0.01
W286A	24 ± 5	4.7 ± 2.0	2.0 ± 0.5	0.4 ± 0.03
Y72A/W286A	24 ± 3	5.8 ± 0.4	2.4 ± 0.46	0.51 ± 0.06
D74N	5 ± 2	0.25 ± 0.07	0.5 ± 0.2	0.92 ± 0.1

[a] Only the lower limit could be estimated due to high background (see Materials and Methods).

of this architecture by replacement of residues E202 (by alanine or glutamine) and E450 (by alanine) results in a substantial reduction in the reactivity of the phosphorylated enzymes toward all three reactivators compared with the wild-type. In most cases, this decrease is a reflection of the lower corresponding k_2 values, suggesting that the perturbation of the active center geometry affects mainly the nucleophilic process. Less pronounced effects can be observed on the affinity of both the phosphorylated and the nonphosphorylated enzymes toward the reactivators tested. This behavior is markedly different from the previously observed effects of replacing Glu202 and Glu450 on the reactivity of HuAChE enzymes toward organophosphates, where affinity rather than nucleophilic efficiency was affected (20, 22, 23).

Effect of amino acid replacements at the PAS on reactivation. Another binding subsite, the PAS, affecting the reactivity properties of the enzyme was mapped at the rim of the gorge, 20 Å from the active site (18, 34–37). Bisquaternary AChE inhibitors bind to the enzyme by bridging the active center and the peripheral anionic site at the rim of the active site gorge (37). TMB-4 and HI-6 are bisquaternary compounds and therefore could be expected to interact simultaneously with the active center and the PAS. In contrast, the monoquaternary 2-PAM is expected to interact only with the active center. Indeed, the affinities of 2-PAM to both the nonphosphorylated and the phosphorylated enzymes were not affected significantly by the PAS mutations Y72A, W286A, and Y72A/W286A (Table 1). Interestingly. a similar pattern of mutational effects on affinity was observed for the bisquaternary HI-6. In contrast, the affinity toward TMB-4 remained relatively unaffected for the free enzymes yet was significantly reduced for the phosphorylated enzymes (≤100- fold in the double mutant Y72A/W286A). This reduction in affinity is the main reason for the pronounced reduction in the corresponding bimolecular rate constants of reactivation by TMB-4 (Table 2). In the case of HI-6, some effects on k_r were also observed, but these are much less pronounced, and the underlying variabilities of K_r and k_2 are less uniform (Table 3). Quite surprisingly, PAS mutations led to a decrease in k_r values for the reactivation by the monopyridinium reactivator 2-PAM. This reduction was not as high as that for TMB-4 but was larger than that for HI-6. Because affinity toward 2-PAM does not change significantly on PAS mutagenesis, the effects on k_r are mainly due to variation in k_2 (Table 1). This observation is intriguing in view of the fact that replacements at positions 72 and 286 have not been observed to affect the chemical reactivity at the active center toward either substrates or covalent and noncovalent inhibitors (18).

Unlike substitution of the other structural elements of the PAS, replacement of Asp74 was shown to affect the binding of charged ligands to the AChE active center (14, 18). This mutation affects the nucleophilic reaction step by the oxime only in the case of HI-6, whereas the k_2 values for 2-PAM and TMB-4 are practically equivalent to those of the wild-type enzyme. This observation underscores the differential effects of PAS mutations on the reactivity toward the individual reactivators, suggesting that the role of PAS in reactivation is more complex than was initially assumed based on the X-ray structure of the 2-PAM/AChE complex.[3]

Discussion

Regeneration of AChE from its phosphoryl adducts, through reactions with oxime reactivators, proceeds much faster than analogous reactions for other phosphorylated enzymes or for low molecular weight organophosphorus model compounds. Such rate acceleration strongly suggests the involvement of the AChE active center in accommodating the oxime reactivator and in facilitating the nucleophilic process. Investigation of the role of the AChE active center in interactions with substrates (14, 16, 17) as well as covalent and noncovalent inhibitors (15, 17, 18, 22) has recently gained momentum with the advent of an experimental approach that combines data from X-ray crystallography, site-directed mutagenesis, enzyme kinetics, and molecular modeling. These studies allowed the elucidation of the functional architecture of the AChE active site gorge and could provide the basis for investigating the more complex interactions of phosphorylated AChE with oxime reactivators.

An adequate measure for probing the effect of mutagenesis on the reactivation process is through comparison of the respective values of the bimolecular rate constants of reactivation (k_r). Such a comparison (Fig. 4) reveals an apparently conserved trend in the effect of the different mutations on reactivation by the three oximes examined. Substitution of residues constituting the hydrophobic pocket (Tyr337, Phe338) had little effect on k_r values, whereas substitution of the H-bond network residues (Glu202, Glu450) and the anionic subside residue (Trp86) resulted in significant decrease in k_r values. Notably, the reactivation rate constants for the three oximes were also affected by replacement of residues at the PAS (Tyr72, Asp74, Trp 286). Although for most mutants carrying residue replacements at the various binding subsites of HuAChE, the variations in k_r values were similar for the three reactivators, closer examination of the kinetic characteristics (according to equation 1) indicated that there were different effects for the different reactivators. The kinetic description, which is supported by the linear relations of $\ln(1 - E_t/E_\infty)$ versus reaction time and of k_{obs} versus 1/[R], allows for the estimation of both the dissociation constants K_r and the rate constants k_2. Altogether, examination of the parameters (Tables 1–3 and Figs. 5 and 6) indicates that the effects of mutagenesis on the different steps of the reactivation process are more complex than they may seem to be based on the corresponding bimolecular rate constants (Fig. 4).

The role of the functional architecture of AChE active center in interaction with ligands is well established. This information is potentially instrumental to understanding the reactivation process provided that the phosphylation of the active site serine does not have a dramatic effect on the structure of the active center. Previous studies have shown, for example, that binding of active center ligands like decidium is not affected by phosphylation of the active site serine (38). One could expect, therefore, that the effects of mutagenesis on the affinity of the free and the phosphorylated enzymes toward the oxime reactivators (as reflected in the values of K_{ox} and K_r, respectively) would be comparable. However, although the affinity of the free enzyme mutants were found to follow the structure-function patterns observed for positively charged noncovalent inhibitors (16, 18), the corresponding affinities of the diethylphosphoryl adducts exhibited a marked variability related to the structure of the specific reactivator. The most pronounced effect on the affinity of the free enzymes was effected by replacement of Trp86, the anionic subsite at the AChE active center, which is crucial for accommodation of charged ligands such as ATC, edrophonium, and decamethonium (16, 18). In addition, like for other charged ligands, mutagenesis at sites related to hydrophobic interactions (Tyr337, Phe338) or acyl pocket accommodation (Phe295, Phe297) on reactivator binding were less dramatic (except for F295A in TMB-4). Nevertheless, a comparison of the dissociation constants (K_r versus K_{ox}) indicates that the mutations have different affects on the affinity of the free and the phosphorylated enzymes toward different reactivators. The most striking difference is the negligible effect of Trp86 replacement on the affinity of the phosphorylated enzyme toward 2-PAM and HI-6 compared with the observed decrease in affinity toward TMB-4. This indicates that the alignment of the reactivators within the active center gorge of the phosphorylated enzyme is markedly different from

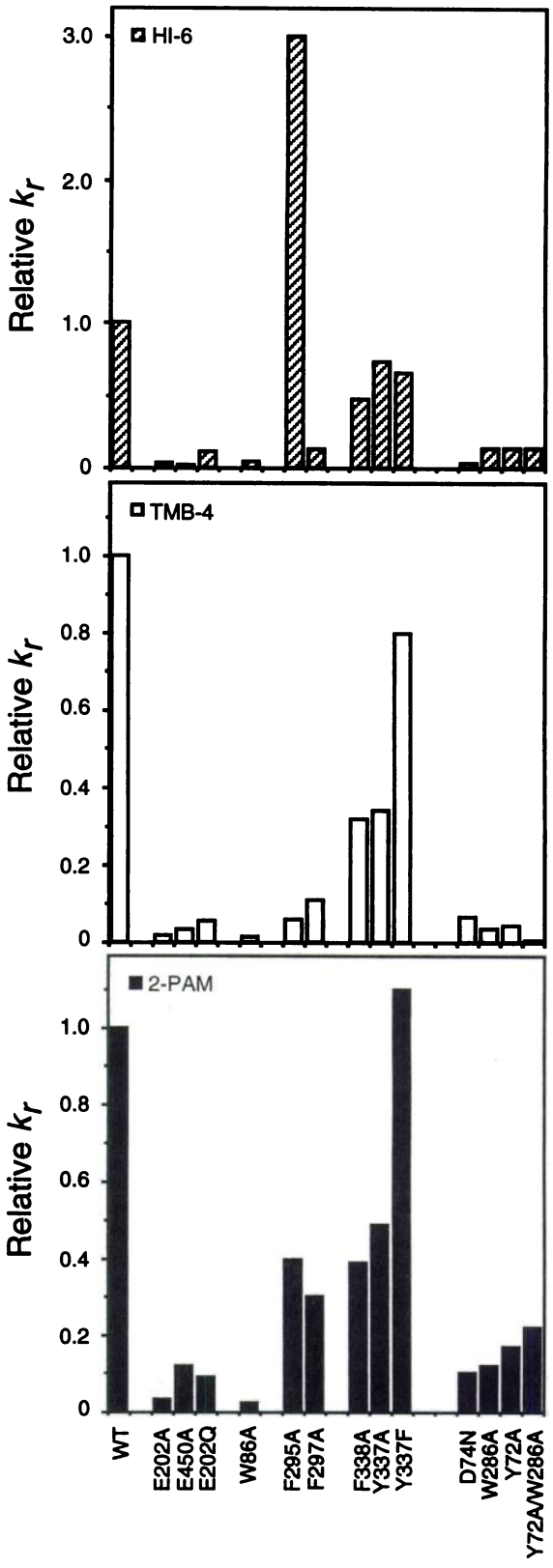

Fig. 4. Relative values of the apparent bimolecular rate constants k_r for reactivation of paraoxon-inhibited HuAChE and its mutant derivatives. The enzymes are grouped according to the subsite at which residue replacement was made: H-bond network (E202A, E202Q, E450A), active center anionic subsite (W86A), acyl pocket (F295A, F297A), hydrophobic pocket (F338A, Y337A, Y337F), and the peripheral anionic site (D74N, W286A, Y72A, Y72A/W286A). *WT*, wild-type.

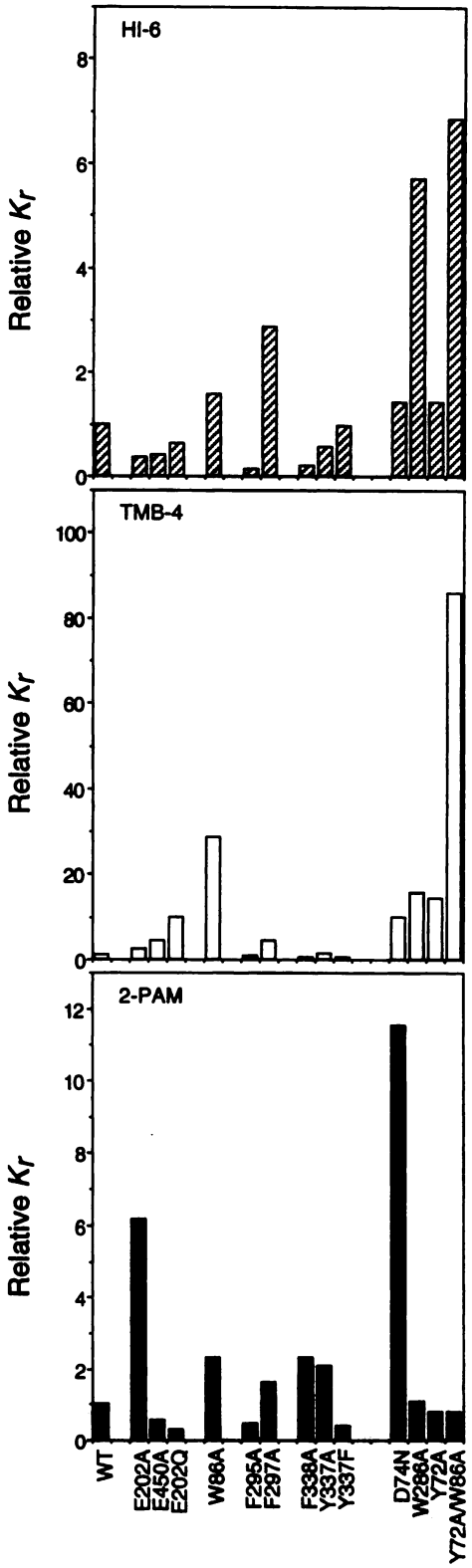

Fig. 5. Relative values of the dissociation constants K_r for oxime reactivator complexes with diethylphosphoryl-HuAChE and its mutant derivative. The enzymes are grouped as shown in Fig. 4. *WT*, wild-type.

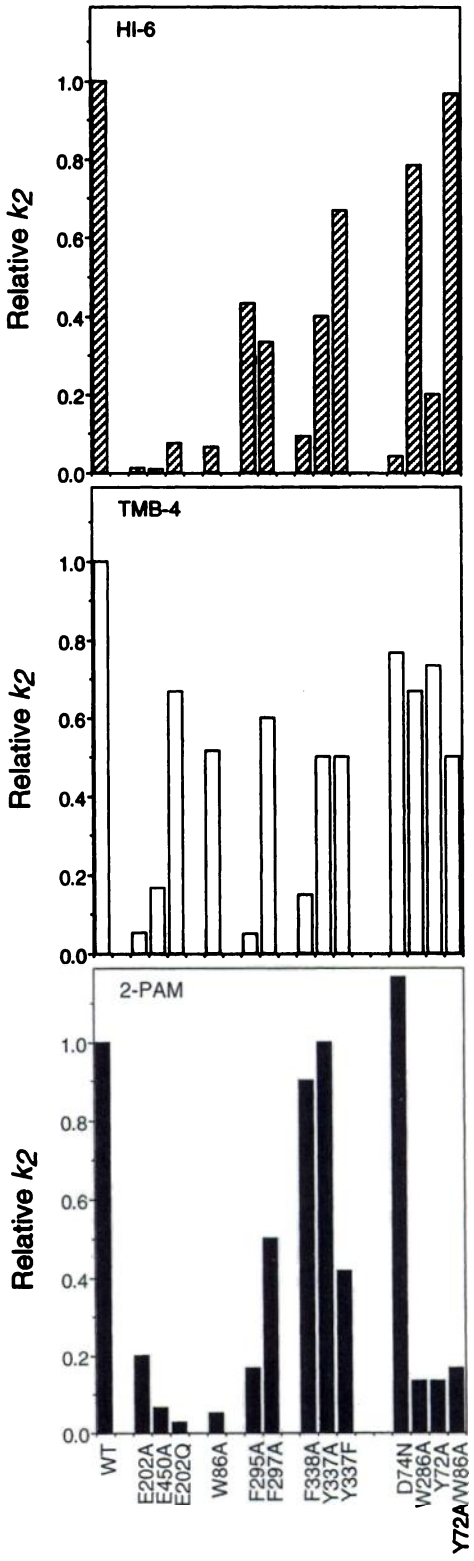

Fig. 6. Relative values of the first-order rate constants k_2 of reactions of oxime reactivator complexes with diethylphosphoryl-HuAChE and its mutant derivative. The enzymes are grouped as shown in Fig. 4. *WT*, wild-type.

that in the free enzyme. Furthermore, distinct oxime reactivators are accommodated differently in the active center. This is substantiated by several other observations: (a) Mutation at position 295 increases the affinity of the phosphorylated enzyme for HI-6 but not for the other reactivators studied. (b) Mutations at position 202 (E202A and E202Q) have different affects on interactions with 2-PAM, HI-6, and TMB-4. (c) Substitution of F338 with alanine results in an

increase in affinity of the phosphorylated enzyme toward HI-6 that is not observed in the free enzyme.

Additional differences in the behavior of different reactivators are related to the effects of PAS mutations on oxime/AChE interactions. Replacements at positions 72 and 286 do not seem to affect the affinity of either the phosphorylated or the free enzymes toward 2-PAM, as expected for a monocharged derivative. Affinities toward the two bispyridinium reactivators are affected by mutations at these PAS positions, yet for HI-6, a decrease in affinity is more pronounced in the free enzyme (~20 fold decrease), whereas for TMB-4, the major effect is observed in the phosphorylated enzymes (18–100-fold). These observations suggest that the PAS could participate in accommodation of one of the charged pyridinium moieties, yet it seems that the two bispyridinium reactivators are differently oriented relative to the functional components of the active center gorge.

Although the PAS seems to be involved in accommodation of the bisquaternary oxime reactivators, its effect on the actual reactivation reaction (as reflected by the rate constants k_2) is not straightforward. Replacements of residues Asp74 and Tyr72 lower the k_2 values for HI-6 while hardly affecting those for TMB-4. On the other hand, mutagenesis at the PAS affects the k_2 values for 2-PAM. The resemblance between the reactivity characteristics of 2-PAM and HI-6, as distinguished from these of TMB-4, are also manifested by the involvement of residue Trp86 as well as of residues constituting the H-bond network (Glu202, Glu450) in the reactivation reaction. The apparent similarity in the reactivity pattern of 2-PAM and HI-6 could be related to the positioning of the oxime moiety on the pyridinium ring relative to the positively charged nitrogen. In 2-PAM and HI-6, the oxime moiety is at position 2, adjacent to the pyridinium nitrogen, whereas in TMB-4, it is located at position 4 (Fig. 1).

Altogether, it is very difficult to rationalize the reactivation process using the previously established functional architecture of the AChE active center gorge (16, 20). Assuming that the overall gorge architecture is not altered significantly by the bound phosphoryl moiety, the observed structure-affinity relationships do not correspond to the defined array of binding elements, including the anionic and hydrophobic subsites as well as the acyl pocket, within the active center gorge. This may indicate that the structures of the reactivator-phosphorylated enzyme complexes are determined primarily by interactions other than those implicated in the corresponding complexes of the free enzyme. One such interaction can involve the oxime and the phosphoryl moieties. This interaction, which is instrumental in properly juxtaposing the two reacting elements, could involve some rearrangements of the gorge, leading to abolishment of the defined binding subsites. These alterations should differ according to the different oxime structure and thus account for some of the oxime-specific effects of the mutagenesis (Tables 1–3).

In conclusion, the experimental approach, which involves site-directed mutagenesis and has been remarkably successful in elucidating the various aspects of AChE reactivity, seems to be less effective in the derivation of the structure-function profile for the reactivation process. One of the major problems in derivation of such profile is that the experimental observations cannot be rationalized in structural terms and are not amenable to molecular modeling because the nature and the extent of the conformational adjustment by the enzyme are not known and are quite difficult to predict. In a recent study, various mutants of mouse AChE were used to analyze reactivation by 2-PAM and HI-6 (24). The authors proposed a model of the phosphonylated AChE/HI-6 complex in which the positive charges of the bisquaternary reactivator were positioned near the indole moieties of Trp86 and Trp286, in the active center and the PAS, respectively. However, such a model may not be applicable to the corresponding reactivation of HuAChE conjugates because the value of the dissociation constant K_r for the HI-6/W86A conjugate complex is practically equivalent to that of the wild-type HuAChE (Table 3). This is quite intriguing in view of the fact that the residue compositions of the active site gorge in HuAChE and mouse AChE are identical (39).

The apparent inconsistency of the kinetic results with the expected structure-function pattern of AChE could indicate the inadequacy of the kinetic model currently used for the reactivation process. Alternatively, the results presented in this study may implicate that interaction of the oxime with the bound phosphyl moieties is indeed the dominant characteristic of the phosphylated AChE/oxime reactivator complexes and/or that the binding modes of oxime to the phosphorylated and nonphosphorylated enzymes are considerably different. In such cases, it is conceivable that reactivation rates could be manipulated by altering the size of the phosphorous alkyl substituents. Specifically, bulkier phosphyl moieties may confer a more restrictive binding environment to the oxime reactivator and thus reveal in greater detail the structure-function characteristics of the reactivation process.

References

1. Chambers, H. W. Organophosphorus compounds: an overview, in *Organophosphates: Chemistry, Fate, and Metabolism* (J. E. Chambers and P. E. Levi, eds.). Academic Press, San Diego, 3–17 (1992).
2. Aldridge, W. N., and E. Reiner. *Enzyme Inhibitors as Substrates*. North-Holland Publishing, Amsterdam (1972).
3. Gray, A. P. Design and structure-activity relationships of antidotes of organophosphorus anticholinesterase agents. *Drug Metab. Rev.* **15**:557-589 (1984).
4. Wilson, B. W., M. J. Hooper, M. E. Hensen, and P. S. Neiberg. Reactivation of organophosphorus inhibited AChE with oximes, in *Organophosphates: Chemistry, Fate, and Metabolism* (J. E. Chambers and P. E. Levi, eds.). Academic Press, San Diego, 108–137 (1992).
5. Ellin, R. I. Anomalies in theories and therapy of intoxication by potent organophosphorus anticholinesterase compounds. *Gen. Pharmacol.* **13**: 457-466 (1982).
6. Taylor, P. Anticholinesterase agents, in *Goodman and Gilman's The Pharmacological Basis of Therapeutics* (A. G. Gilman, T. W. Rall, A. S. Nies, and P. Taylor, eds.). Pergamon Press, Chapter 7 (1990).
7. Rousseaux, C. G., and A. K. Dua. Pharmacology of HI-6, an H-series oxime. *Can. J. Physiol. Pharmacol.* **67**:1183-1189 (1989).
8. Eyer, P., I. Hagedorn, R. Klimmek, P. Lippstreu, M. Löffeler, H. Oldiges, U. Spöhrer, I. Steidl, L. Szinicz, and F. Worek. HLö 7 dimethanesulfonate: a potent bispyridinium-dioxime against anticholinesterases. *Arch. Toxicol.* **66**:603-621 (1992).
9. Clement, J. G., S. Rosario, E. Bessette, and N. Erhardt. Soman and sarin inhibition of molecular forms of acetylcholinesterase in mice. *Biochem. Pharmacol.* **42**:329-335 (1991).
10. Sussman, J. L., M. Harel, F. Frolow, C. Oefner, A. Goldman, and I. Silman. Atomic structure of acetylcholinesterase from *Torpedo californica*: a prototypic acetylcholine binding protein. *Science (Washington D. C.)* **253**:872-879 (1991).
11. Gibney, G., S. Camp, M. Dionne, K. MacPhee-Quigley, and P. Taylor. Mutagenesis of essential functional residues in acetylcholinesterase. *Proc. Natl. Acad. Sci. USA* **87**:7546-7550 (1990).
12. Shafferman, A., C. Kronman, Y. Flashner, M. Leitner, H. Grosfeld, A. Ordentlich, Y. Gozes, S. Cohen, N. Ariel, D. Barak, M. Harel, I. Silman, J. L. Sussman, and B. Velan. Mutagenesis of acetylcholinesterase: identification of residues involved in catalytic activity and in polypeptide folding. *J. Biol. Chem.* **267**:17649-17648 (1992).
13. Harel, M., J. L. Sussman, E. Krejci, S. Bon, P. Chanal, J. Massoulie, and I. Silman. Conversion of acetylcholinesterase to butyrylcholinesterase: modeling and mutagenesis. *Proc. Natl. Acad. Sci. USA* **89**:10827-10831 (1992).

14. Shafferman, A., B. Velan, A. Ordentlich, C. Kronman, H. Grosfeld, M. Leitner, Y. Flashner, S. Cohen, D. Barak, and N. Ariel. Substrate inhibition of acetylcholinesterase: residues involved in signal transduction from the surface to the active center. *EMBO J.* **11**:3561-3568 (1992).
15. Vellom, D. C., Z. Radic, Y. Li, N. A. Pickering, S. Camp, and P. Taylor. Amino acid residues controlling acetylcholinesterase and butyrylcholinesterase specificity. *Biochemistry* **32**:12–17 (1993).
16. Ordentlich, A., D. Barak, C. Kronman, Y. Flashner, M. Leitner, Y. Segall, N. Ariel, S. Cohen, B. Velan, and A. Shafferman. Dissection of the human acetylcholinesterase active center, determinants of substrate specificity. *J. Biol. Chem.* **268**:17083-17095 (1993).
17. Taylor, P., and Z. Radic. The cholinesterases: from genes to proteins. *Annu. Rev. Pharmacol. Toxicol.* **34**:281-320 (1994).
18. Barak, D., C. Kronman, A. Ordentlich, N. Ariel, A. Bromberg, D. Marcus, A. Lazar, B. Velan, and A. Shafferman. Acetylcholinesterase peripheral anionic site degeneracy conferred by amino acid arrays sharing a common core. *J. Biol. Chem.* **269**:6296-6305 (1994).
19. Gnatt, A., Y. Loewenstein, A. Yaron, M. Schwartz, and H. Soreq. Site-directed mutagenesis of active site residues reveals plasticity of human butyrylcholinesterase in substrate and inhibitor interactions. *J. Neurochem.* **62**:749-755 (1994).
20. Ordentlich, A., D. Barak, C. Kronman, N. Ariel, Y. Segall, B. Velan, and A. Shafferman. Contribution of aromatic moieties of tyrosine 133 and of the anionic subsite tryptophan 86 to catalytic efficiency and allosteric modulation of acetylcholinesterase. *J. Biol. Chem.* **270**:2082-2091 (1995).
21. Radic, Z., R. Duran, D. C. Vellom, Y. Li, C. Cervenanski, and P. Taylor. Site of fasciculin interaction with acetylcholine. *J. Biol. Chem.* **269**:11233-11239 (1994).
22. Ordentlich, A., D. Barak, C. Kronman, N. Ariel, Y. Segall, B. Velan, and A. Shafferman. The architecture of human acetylcholinesterase active center probed by interactions with selected organophosphate inhibitors. *J. Biol. Chem.* **271**:11953-11962 (1996).
23. Ordentlich, A., C. Kronman, D. Barak, D. Stein, N. Ariel, D. Marcus, B. Velan, and A. Shafferman. Engineering resistance to 'aging' of phosphylated human acetylcholinesterase. *FEBS Lett.* **334**:215-220 (1993).
24. Ashani, Y., Z. Radic, I. Tsigelny, D. C. Vellom, N. A. Pickering, D. M. Quinn, B. P. Doctor, and P. Taylor. Amino acid residues controlling reactivation of organophosphonyl conjugates of acetylcholinesterase by mono- and bisquaternary oximes. *J. Biol. Chem.* **270**:6370-6380 (1995).
25. Velan, B., H. Grosfeld, C. Kronman, M. Leitner, Y. Gozes, A. Lazar, Y. Flashner, D. Markus, S. Cohen, and A. Shafferman. The effect of elimination of intersubunit disulfide bonds on the activity, assembly, and secretion of recombinant human acetylcholinesterase. *J. Biol. Chem.* **266**: 23977-23984 (1991).
26. Kronman, C., B. Velan, Y. Gozes, M. Leitner, Y. Flashner, A. Lazar, D. Marcus, T. Sery, A. Papier, H. Grosfeld, S. Cohen, and A. Shafferman. Production and secretion of high levels of recombinant human acetylcholinesterase. *Gene* **121**:295-304 (1992).
27. Lazar, A., S. Reuveny, C. Kronman, B. Velan, and A. Shafferman. Evaluation of anchorage-dependent cell propagation systems for production of human acetylcholinesterase by recombinant 293 cells. *Cytotechnology* **13**: 115-123 (1993).
28. Barak, D., A. Ordentlich, A. Bromberg, C. Kronman, D. Marcus, A. Lazar, N. Ariel, B. Velan, and A. Shafferman. Allosteric modulation of acetylcholinesterase activity by peripheral ligands involves a conformational transition of the anionic subsite. *Biochemistry* **34**:15444-15452 (1995).
29. Ellman, G. L., K. D. Courtney, V. Andres, and R. M. Featherstone. A new and rapid colorimetric determination of acetylcholinesterase activity. *Biochem. Pharmacol.* **7**:88-95 (1961).
30. Green, A. L., and H. J. Smith. The reactivation of cholinesterase inhibited organophosphorus compounds. *Biochem. J.* **68**:28-31 (1958).
31. Main, A. R. Affinity and phosphorylation constants for the inhibition of esterases by organophosphates. *Science (Washington D. C.)* **144**:992-993 (1964).
32. Harvey, B., R. P. Scott, D. J. Sellers, and P. Watts. *In vitro* studies on the reactivation by oximes of phosphylated acetylcholinesterase-II. *Biochem. Pharmacol.* **35**:745-751 (1986).
33. Whiteley, C. G., and D. S. Ngwenya. Protein ligand interactions: alkylated pyridinium salts as inhibitors of acetylcholinesterase from *Electrophorus electricus*. *Biochem. Biophys. Res. Commun.* **211**:1083-1090 (1995).
34. Berman, H. A., W. Becktel, and P. Taylor. Spectroscopic studies on acetylcholinesterase: influence peripheral-site occupation on active-center conformation. *Biochemistry* **20**:4803-4810 (1981).
35. Hucho, F., J. Jarv, and C. Weise. Substrate-binding sites in acetylcholinesterase. *Trends Pharmacol. Sci.* **12**:422-427 (1991).
36. Radic, Z., E. Reiner, and P. Taylor. Role of the peripheral binding site on acetylcholinesterase: inhibition by substrates and coumarin derivatives. *Mol. Pharmacol.* **39**:98-104 (1991).
37. Harel, M., I. Schalk, L. Ehret-Sabatier, F. Bouet, M. Goeldner, C. Hirth, P. H. Axelsen, I. Silman, and J. L. Sussman. Quaternary ligand binding to aromatic residues in the active-site gorge of acetylcholinesterase. *Proc. Natl. Acad. Sci. USA* **90**:9031-9035 (1993).
38. Berman, H. A., and M. M. Decker. Kinetic, equilibrium and spectroscopic studies on cation association at the active center of acetylcholinesterase: topographic distinction between trimethyl and trimethylammonium sites. *Biochim. Biophys. Acta* **872**:125-133 (1986).
39. Gentry, M. K., and Doctor, B. P. Amino acid alignment of cholinesterases, esterases, lipases and related proteins, in *Enzymes of the Cholinesterase Family* (D. M. Quinn, A. S. Balasubarmanian, B. P. Doctor, and P. Taylor, eds.). Plenum Publishing, New York, 493–505 (1995).
40. Bourne, N., and A. Williams. Evidence for a single transition state in the transfer of the phosphoryl group ($-PO_3^{2-}$) to nitrogen nucleophiles from pyridino-N- phosphonates. *J. Am. Chem. Soc.* **106**:7591-7596 (1984).
41. Massoulie, J., J. L. Sussman, B. P. Doctor, H. Soreq, B. Velan, M. Cygler, R. Rotundo, A. Shafferman, I. Silman, and P. Taylor. Recommendations for nomenclature in cholinesterases, in *Multidisciplinary Approaches to Cholinesterase Functions* (A. Shafferman and B. Velan, eds.). Plenum Publishing, New York, 285–288 (1992).

Send reprint requests to: Dr. Avigdor Shafferman, Israel Institute for Biological Research, Ness-Ziona 70450, Israel. E-mail: wxiibr@weizmann.weizmann.ac.il